AD_____

Award Number: W81XWH-09-1-0726

TITLE: CINRG: Systems Biology of Glucocorticoids in Muscle Disease

PRINCIPAL INVESTIGATOR: Zuyi Wang, Ph.D.

CONTRACTING ORGANIZATION: Children's Research Institute
Washington, DC 20010

REPORT DATE: October 2013

TYPE OF REPORT: Final

PREPARED FOR: U.S. Army Medical Research and Materiel Command
Fort Detrick, Maryland 21702-5012

DISTRIBUTION STATEMENT: Approved for public release; distribution unlimited

REPORT DOCUMENTATION PAGE

Form Approved
OMB No. 0704-0188

1. REPORT DATE *(DD-MM-YYYY)*	2. REPORT TYPE	3. DATES COVERED *(From - To)*
October 2013	Final	21 September 2009 - 20 September 2013

4. TITLE AND SUBTITLE
CINRG: Systems Biology of Glucocorticoids in Muscle Disease

5a. CONTRACT NUMBER

5b. GRANT NUMBER
W81XWH-09-1-0726

5c. PROGRAM ELEMENT NUMBER

6. AUTHOR(S)
Zuyi Wang, Ph.D.

E-Mail: zwang@childrensnational.org

5d. PROJECT NUMBER

5e. TASK NUMBER

5f. WORK UNIT NUMBER

7. PERFORMING ORGANIZATION NAME(S) AND ADDRESS(ES)
Children's Research Institute
Washington, DC 20010

8. PERFORMING ORGANIZATION REPORT NUMBER

9. SPONSORING / MONITORING AGENCY NAME(S) AND ADDRESS(ES)
U.S. Army Medical Research and Materiel Command
Fort Detrick, Maryland 21702-5012

10. SPONSOR/MONITOR'S ACRONYM(S)

11. SPONSOR/MONITOR'S REPORT NUMBER(S)

12. DISTRIBUTION / AVAILABILITY STATEMENT
Approved for Public Release; Distribution Unlimited

13. SUPPLEMENTARY NOTES

14. ABSTRACT

We developed two computational network reconstruction methods, linear state space model and dynamic Bayesian network, to infer transcriptional networks using the rat acute transcriptional time series of bolus administration of glucocorticoids. This time series was re-profiled using Illumina gene expression BeadChip for a much broader coverage. We have successfully used staged injection models to induce asynchronous regenerations in normal mouse muscles. Using laser capture microscopy and gene expression microarray profiling, we extensively analyzed muscle tissues dissected from the injection sites and in between regions in the 4 day and 10 day reinjury series. The results showed inappropriate crosstalk in the muscles from in between areas due to neighboring asynchronous regenerations in both injection series. We showed that daily administration of Prednisolone suppressed inappropriate crosstalk in the muscle regions between asynchronously remodeling areas. We have been awarded several new grants focusing on studying glucocorticoid mechanism in treating DMD and asthma. Two doctoral students graduated or are graduating under partial support from this grant.

15. SUBJECT TERMS
Duchenne Muscular dystrophy, Glucocorticoids, Systems biology, Drug mechanism

16. SECURITY CLASSIFICATION OF:			17. LIMITATION OF ABSTRACT	18. NUMBER OF PAGES	19a. NAME OF RESPONSIBLE PERSON
a. REPORT	b. ABSTRACT	c. THIS PAGE			USAMRMC
U	U	U	UU	18	19b. TELEPHONE NUMBER *(include area code)*

Table of Contents

Final progress report (2009-2013) for Contract W81XWH-09-1-0726

SYSTEMS BIOLOGY OF GLUCOCORTICOIDS IN MUSCLE DISEASE

Introduction

Duchenne muscular dystrophy (DMD) is the most common and incurable muscular dystrophy of childhood. Muscle regeneration fails with advancing age, leading to considerable fibrosis. Corticosteroid therapy in DMD has been shown to improve muscle strength and function both acutely and over long-time frames. The molecular mechanisms explaining the beneficial effect of glucocorticoids is unknown; and the beneficial response of DMD patients is enigmatic due to the deleterious wasting effects chronic glucocorticoids have on normal muscle. The goal of this proposal is to use computational systems biology approach to model the molecular responses, and to extend and validate the integration of signaling and transcriptional networks using our pre-existing high throughput mouse and rat data sets of transcriptional, proteomic, and PK/PD response to glucocorticoids and human neuromuscular diseases. We also use laboratory approaches to test the hypothesis that the effect of glucocorticoids on reducing inappropriate cross-talk in TGFβ networks improves muscle regeneration. We anticipate that the computational models and experimental results resulted from the proposed research will provide a novel model for efficacy of steroids in DMD.

Body

Progress of Specific Aim 1

Specific Aim 1. Provide a multi-scale computational model on the integrated acute proteome (signaling) and transcriptional response regarding metabolic remodeling and TGFβ cascades in muscle induced by glucocorticoids under bolus administration of glucocorticoids. (August 2009 – December 2010)

Development of proposed linear state space model for genetic network reconstruction. (Year 1, 2, 3 and 4)

We developed a prototype of the proposed wavelet/linear state space model. As described in the proposal, this approach consists of two components. The first component is gene modulization by wavelet feature extraction, extracting transient features using wavelet transform [1-3] from time series signals and modulizing the genes. The second component is molecular network construction, in which we estimate the structure and parameters of a molecular network to quantify the interaction relationships among the identified genes/gene modules. In the proposal, we planned to use two alternative approaches for the second component. Approach A uses dynamic Bayesian network (DBN) to estimate the parameters and conditional probability distributions in Eq. (1) [4-9] (reported in the following section). Our newly proposed Approach B uniquely combines wavelet transform (trend transform) and linear regression for estimating the parameters of the linear regulation model (Eq. (2)).

$$\mathbf{Y}_{t+1} = \mathbf{G}\mathbf{Y}_t + \mathbf{K}\mathbf{U}_t + \mathbf{W}_t, \left(t = 1,2,...T-1\right) \quad (1)$$

$$\mathbf{X}_{t+1} = \mathbf{G}\mathbf{X}_t + \mathbf{K}\mathbf{U}_t, \mathbf{Y}_t = \mathbf{C}\mathbf{X}_t + \mathbf{W}_t, \left(t = 1,2,...T-1\right) \quad (2)$$

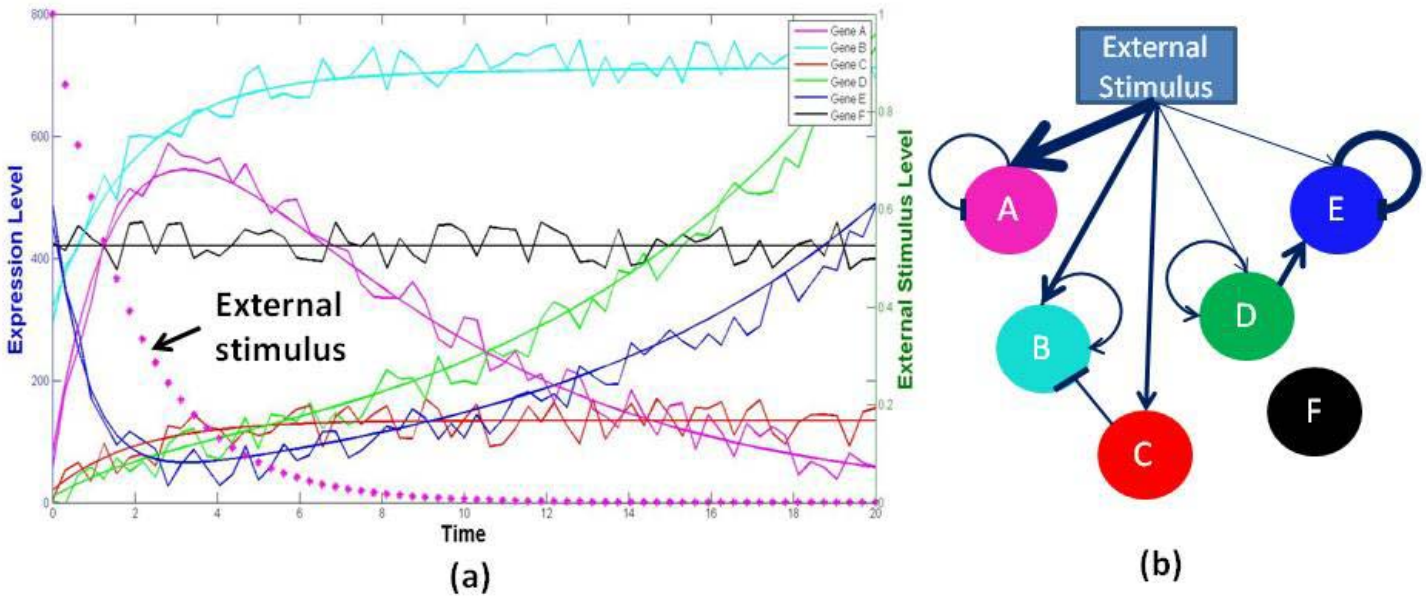

Figure 2. Simulation experiment on genetic network reconstruction using Approach B wavelet/linear regulation model. (a) Simulated gene expression of six genes and an external stimulus. (b) The regulatory relationship among the genes and the external stimulus. The weight of the lines indicates the strength of regulation.

We developed and tested the combined wavelet analysis and linear regression method (Approach B) on simulated data, and obtained promising results. We generated an interaction model (Figure 2b) consisting of six genes (each with a times sequence representing its change in response to an external stimulus) according to the linear Markov model with given parameters and an external stimulus. We simulated different types of the regulatory relationship among the genes and the external stimulus, including positive stimulation and negative inhibition, self-stimulation and self-inhibition, and gene with no interaction with all others (Figure 2b). The thickness of the lines indicates the regulatory strength (regulatory coefficient). Random noises were also added to each signal. Then, we used this method to estimate the regulatory coefficients using the *noisy* signals (i.e., **G**, and **K** in Eq. (2) for wavelet/linear regression). Finally, we used the estimated coefficients to reconstruct the signals, and compared them to the original signals. The closer the reconstructed signals (smooth curves, without noise) are to the original signals (fluctuating curves, with noise embedded), the better the parameters are estimated. Figure 2a shows that our wavelet/linear state space method accurately reconstructed the signals, and precisely estimated the regulatory strength. The results agree with our expectation that Approach B effectively reduces the impact of large amount of noise and capture change patterns, which makes the estimation of the regulatory strength and relationship more precise. This part of the project is still ongoing; we are testing Approach B on the re-profiled rat acute transcriptional time series of bolus administration of glucocorticoids.

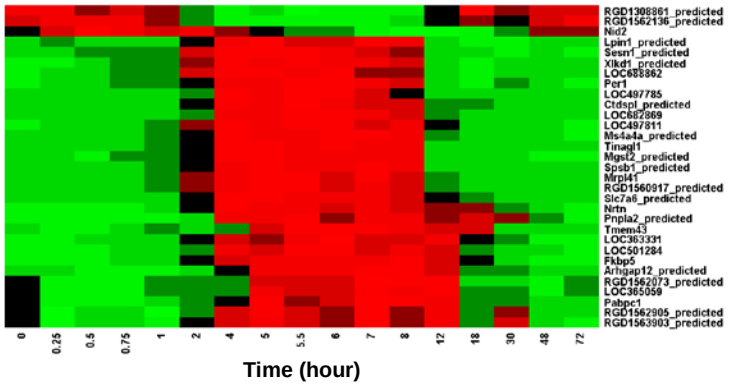

Figure 1. Heat map of some transcripts that are contained in Illumina gene expression chip but not in Affymetrix chip and are significantly affected by glucocorticoids. Red color indicates up-regulated, and green for down-regulated.

Re-profiling of rat acute transcriptional time series of bolus administration of glucocorticoids using Illumina BeadArray gene expression chip. (Year 2)

In order to effectively infer transcriptional networks, we have re-profiled the samples of the rat acute transcriptional time series of bolus administration of glucocorticoids using Illumina gene expression BeadArray chips. The cost was covered by a different funding resource. The old time series data were generated using Affymetrix U34A chip a number of years ago, this outdated chip contains only 5138 unique gene (8740 probe sets) while the new Illumina BeadChip contains 21675 unique genes/probes. From our initial analysis of the new Illumina time series, we have found many genes that are affected by glucocorticoids are in the Illumina chip but not in the old Affymetrix U34A chip (Figure 1 shows some examples). Although both state space model and Bayesian networks we used in our network reconstruction approach can use hidden variables to represent possible factors contributing to regulatory interactions that are not measured, introducing excessive hidden variables may significantly increase the risk of model over-fitting. Given a larger number of measured transcripts in the new time series, we expect that we will obtain more reliable and complete network results.

Development of proposed dynamic Bayesian network for genetic network reconstruction. (Year 3)

We have also developed Approach A, dynamic Bayesian network (DBN), and we are applying it to reconstructing genetic networks based on the rat muscle acute or chronic glucocorticoid transcriptional time series data sets. DBN is a graphical model of repeated segments to represent stochastic process. A DBN with hidden Markov model is illustrated in Figure 3. DBN is the most advanced tool for analyzing dynamic process and building dynamic probabilistic model. We will use DBN with the Markov model to analyze the regulatory effects of genes represented in the transcriptional time series. Note that each node in Figure 3 represents a vector of variables, e.g., external stimuli, hidden state variables, or observations.

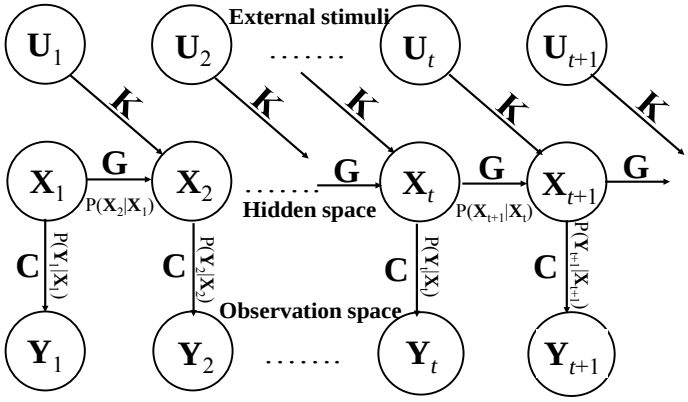

Figure 3. A general diagram of dynamic Bayesian network.

DBN has a number of advantages. It is suitable to model complex hierarchical relationships and relationships with nonlinear properties using dynamic time series data. In addition, DBN does not make any restrictive assumptions such as independency among variables and linear interaction. On the contrary, DBN faithfully evaluates all possible regulatory network structures and identifies the most optimal one that is best supported by the data. Therefore, DBN does not suffer from common problems existing in most conventional statistical methods, such as confounding variables.

Despite the important advantages of Bayesian network method, it has a major challenge, it demands a large sample size that is often hard to obtain.[10-12] To maintain a balance between variable size and sample size and avoid overfitting, we selected salient variables that have the strongest influence on the outcomes of interest based on the mutual information criterion, $m(X,Y) = \sum_{x,y} P(x,y) \log\left[\frac{P(x,y)}{P(x)P(y)}\right]$, where $P(x,y)$, $P(x)$, and $P(y)$ are, respectively, the joint and marginal probabilities of variable X and Y, and X and Y are variable and outcome. If variable X is independent from outcome, Y, the mutual information is zero. The larger the mutual information is, the stronger the influence of X on Y is. Because that we are modeling a dynamic process, we use the generalized mutual information $m(X,Y) = \sum_{t=1}^{T} \sum_{x,y} P_t(x,y) \log\left[\frac{P_t(x,y)}{P_t(x)P_t(y)}\right]$, where $P_t(x,y)$, $P_t(x)$, and $P_t(y)$ are, respectively, the joint and marginal probability of variable X and Y at time point t. This generalized mutual information given equal weight to those at every time point. We are trying to select a set of variables according to the available number of samples and time points in the time series, so that our DBN model has a sound statistical support by the available samples. Moreover, we have developed a novel variable ranking and

selection method, the Bayesian Network with Variable Combination (BNVC).[13] We will also use BNVC to rank the candidate input variables (genes) and select the variables that have the strongest influence on the desired outcomes.

We are using the recently developed DBN software to analyze the rat muscle acute or chronic glucocorticoid transcriptional time series data sets. The main results are the transition matrix $P_t(\boldsymbol{X}_{t+1}|\boldsymbol{X}_t)$ where $\boldsymbol{X}_t$ is the set of selected variables (genes) at time point, t. The transition matrix is the probabilistic trajectory, and it describes the regulatory effect of selected variables (genes) at the current time point on the values of variables (genes) at the next time point. With the transition matrix, we can derive genetic regulatory networks.

Progress of Specific Aim 2

Specific Aim 2. Model the beneficial effects of daily bolus vs. detrimental effects of chronic administration of glucocorticoids.

As discussed above, since we recently re-profiled the rat acute transcriptional time series set and two computational network reconstruction algorithms, we are working on network reconstruction using the new time series and the algorithms. The results will be needed to complete the proposed work in Aim 2, the work on Aim 2 is ongoing.

Identification of commonly shared canonical pathways related to DMD pathogenesis at different age/disease stages across human DMD, and mouse and dog models of DMD. (Year 2)

Aim 2d is to find which genes potentially lead to asynchronous regeneration in Duchenne muscle and how glucocorticoids rescue the issue. The more we study on this topic, the more we realize that it is important to trace the upstream of the disease pathogenesis, i.e., the genes that are affected in the early or presymptomatic stage (such as fetus or infant) and may become seeds leading to broader molecular deregulation. Studying these upstream genes not only will increase our understanding of how the disease is initiated and develop, but also it is important for design better glucocorticoids regimen.

Our lab has multiple muscle transcriptional profiling data sets of human DMD, and animal DMD animal models (e.g., mouse mdx, and dog GRMD (Golden Retriever Muscular dystrophy)) that contain subjects of different age stages (see list below). Based on these data, we have identified a series of commonly shared canonical pathways related to DMD pathogenesis at different age/disease stages across human, mouse and dog (Table 1). Two age stages are matched across human, mouse and dog: presymptomatic/young stage (human 0-2 year-old, mouse 1 week-old, dog 4-9 week-old), postsymptomatic/old stage (human 2-10 year-old, mouse 3 week-old, dog 6 month-old).

List of transcriptional data sets used in this analysis:

1. Multi-group human neuromuscular diseases: 10 groups, 109 samples, profiled on Affymetrix Human Genome U133 plus 2.0 microarray. The data set includes DMD and control subjects.
2. Early stage human DMD muscle time series: control and DMD fetus and infant subjects, total 11 samples, profiled on Affymetrix Human Genome U95Av2 microarrays.
3. Mdx mouse early muscle necrosis time series: wild type and mdx mice, 4 age groups (5 days, 2, 3, and 6 weeks), total 24 samples, profiled on Affymetrix Mouse Genome 430 v2.0 microarray.
4. GRMD dog muscle time series: wild type and GRMD dogs, 3 muscle types (vastus lateralis, cranial sartorius, long digital extensor), 2 age groups (4-9 weeks and 6 months), total 72 samples, profiled on Affymetrix Canine Genome 2.0 microarray.

Table 1. List of commonly shared canonical pathways related to DMD pathogenesis at different age/disease stages across human, mouse and dog.	
Production of Nitric Oxide and Reactive Oxygen Species in Macrophages	GM-CSF Signaling
Germ Cell-Sertoli Cell Junction Signaling	PI3K Signaling in B Lymphocytes
Leukocyte Extravasation Signaling	Actin Cytoskeleton Signaling
LXR/RXR Activation	RhoA Signaling
Antigen Presentation Pathway	Ephrin Receptor Signaling
Molecular Mechanisms of Cell Proliferation	IL-4 Signaling
Role of NFAT in Muscle Hypertrophy	Cellular Effects of Sildenafil (Viagra)
α-Adrenergic Signaling	VEGF Signaling
Integrin Signaling	Complement System
Fibrosis	HGF Signaling
P2Y Purigenic Receptor Signaling Pathway	FcY Receptor-mediated Phagocytosis in Macrophages and Monocytes
Sphingosine-1-phosphate Signaling	fMLP Signaling in Neutrophils
Nitric Oxide Signaling in Muscle	Regulation of Actin-based Motility by Rho
IGF-1 Signaling	

All of the listed pathways (Table 1) are sporadically or not affected at the presymptomatic stage in human, mouse and dog, but they are much more broadly affected at the postsymptomatic stage.

Progress of Specific Aim 3

Specific Aim 3. Development of experimental model of asynchronous muscle regeneration.

Repeated injury to induce asynchronous regeneration in normal mouse muscle. (Year 1, 2, 3, and 4)

We reasoned that a potential experimental model to test asynchronous regeneration would be to induce localized regions of muscle degeneration and regeneration in wild type mice, with repetitive regional bouts at defined time points. We have tested and compared several different experimental models of multiple staged injections of notexin for inducing asynchronous (Figure 4). To date, 13 mice were bilaterally injected in gastrocnemii, with 0, 1, 2, 4, 5, or 10 days between the first and second injections (at least 2 mice/group). The mice were given BrdU on the third day after the second injection, and were sacrificed 13 days after the second injection (the time when regeneration due to the second injection should largely complete). The purpose of this spacing was to see if the stage of the regenerating muscle from the first

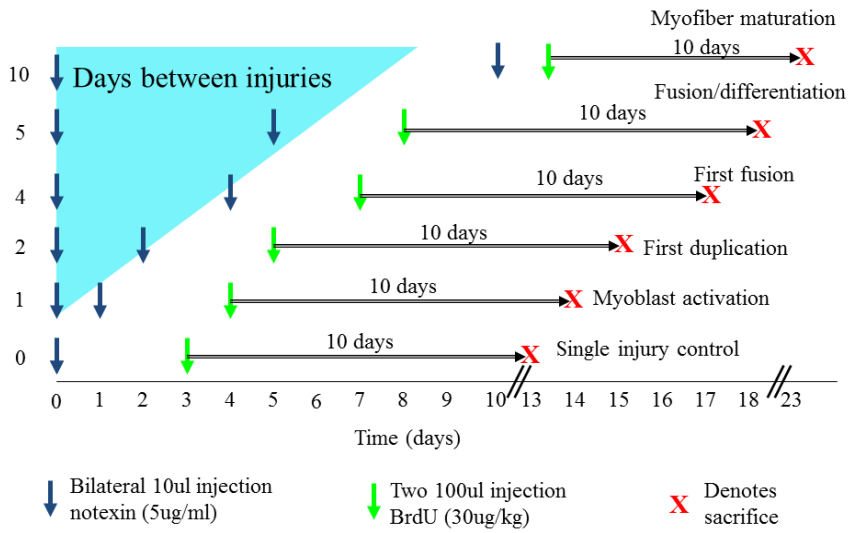

Figure 4. Study design for feasibility test of repeated injections for inducing asynchronous regeneration in normal mouse muscle. As indicated in the figure, spacing between the two injections was designed based on interfering with specific stages of regeneration by the second injection/injury.

injury resulted in different effects on the second injury. The stages of the first injury when the second injection was place were myoblast activation, myoblast proliferation, myoblast differentiation, myotube fusion, and myotube maturation, respectively.

Placement of repeated injection of notexin to muscles.

We learned a few methods that are important for giving proper repeated injections of notexin to muscles. We found that dipping the needle in tattoo dye resulted in the surface of the gastrocnemius being covered in dye. The dye on the muscle surface interfered with our ability to place the successive injection accurately because we could not see the original insertion site and only portions of the injection tract through the muscle. Additionally, the tattoo dye on the surface of the muscle dried into a layer of plastic that inhibited proper wound healing. Although we were able to remove the majority of this excess dye during the second surgery, the skin of some of the animals did not heal together properly. This may have also caused an immune reaction and slowed the muscle regeneration – it is not possible for us to determine the specific effects the excess tattoo dye had. As a result of these two complications, analyzing the tissues has been an extremely slow process.

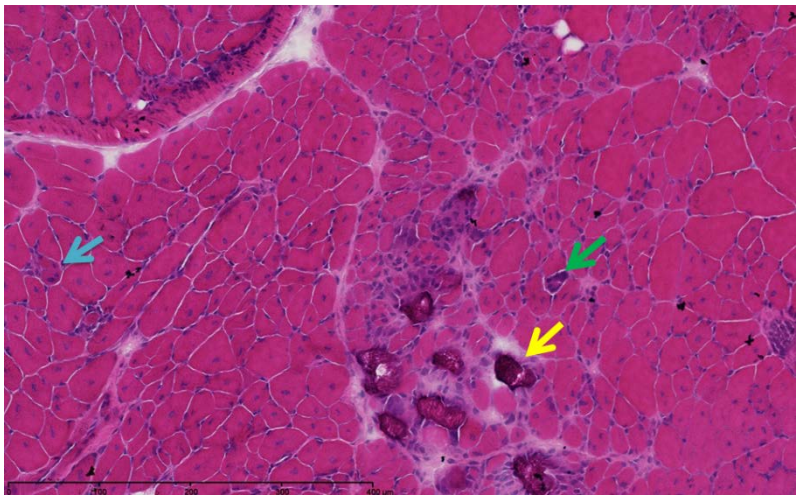

Figure 5. Simultaneous muscle regeneration and degeneration observed in repeated injuried muscles. This gastrocnemius from the day 10 reinjury model/group still had regeneration and degeneration at 13 days after the second injury. Normal muscles with single injury should almost fully regenerate at this stage. However, in this case, there is an increase in degenerating fibers (yellow arrow) and regeneration is still ongoing: presence of myoblast fusion (blue arrow) and dividing myoblasts (green arrow).

Importantly, we have found that we cannot be sure if the tissue section we are analyzing has been damaged more than once. Based on all of these observations, we mixed tattoo dye with the notexin and injected into the muscle. While dye dispersion through the tissue may not be to the same extent as the notexin, the dye will mark at least a portion of the tissue damaged. Each round of damage will be marked with a different color tattoo dye to enable us to distinguish regions of regeneration. Including the tattoo dye in the injection material will guarantee that the area of the tissue being analyzed has overlapping regions of regeneration because we will be able to see more than one color of dye particles. Notably, we have tested the tattoo dyes and found that they do not interfere with fluorescent immunohistochemical analysis of regeneration.

Evidences that show repeated injection induced muscle injuries and asynchronous muscle regeneration in normal mouse muscles

Using the gastrocnemii isolated from the repeated injection area, we sectioned the tissues for histological analysis. We analyzed the images from H&E, Van Gieson, and BrdU stained slides, and this work is still ongoing. Based on the following evidences, our initial analysis showed that we have successfully interfered with the regeneration process in muscles from the groups where the second injection occurred during a later stage of regeneration (e.g. 10 day reinjury group).

1. The tissues that should be completely regenerated were still undergoing rounds of regeneration (Figure 5)
2. An increase in degenerating fibers was found in groups with more than one day between injections (Figure 6).
3. We evaluated fiber diameter sizes, focusing solely on the fibers that have regenerated at least one time (we measured only fibers with centralized nuclei). We found that the 10 day reinjury group had smaller fibers and more of these small fibers than any other group, while still maintaining larger fibers. This greater range in fiber sizes mimics what is seen in patients with DMD (Figure 6).

4. We used Van Gieson staining to visualize connective tissue, and to determine if any of the reinjury groups have an increase incidence of fibrosis. Cursory examination suggests that the muscle of the

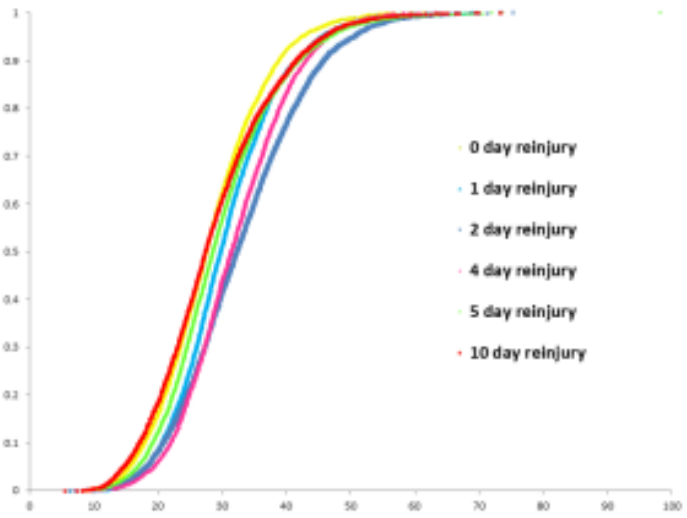

Figure 6. Cumulative frequency distribution of centrally nucleated fibers shows that 10 day reinjury group has the smallest and largest range of fibers. y-axis is cumulative frequency distribution, x-axis is Feret's minimum diameter (um).

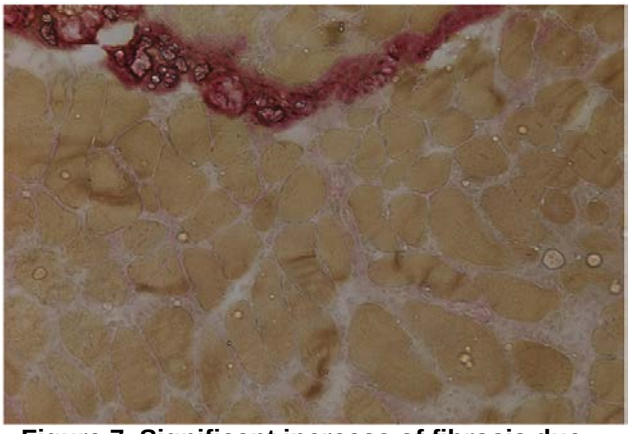

Figure 7. Significant increase of fibrosis due to repeated injuries. Considerable fibrosis (light pink staining between fibers and dark red) exists in this image of gastrocnemius from an 8 wk old BL6 mouse from the day 10 reinjury group. Although the analysis of the Van Gieson data is in progress, the preliminary data suggest there is a significant increase in fibrosis in the day 10 reinjury group over groups with 2 or fewer days between injuries.

reinjury groups with more days in between two injuries have an increase in collagen (Figure 7).

5. Fibrosis is a major concern in DMD muslces because fibroblasts migrate into the muscle tissue and replace the area that had been used to generate contractile force with connective tissue. In order to determine if the timing of the reinjury affects the amount of fibrosis, we performed Van Gieson staining to measure the amount of interstitial connective tissue present in muscle sections. We analyzed the images of the stained muscle sections using Image software to determine the percentage of muscle tissue per image field that is occupied by connective tissue. We found that the 10 day reinjury group has the greatest increase in connective tissue compared to other groups (Figure 8). The 5 day injury group also had an increase in interstitial connective tissue. Next, we tried to determine if this change in connective tissue was permanent. When connective tissue becomes a permanent fixture of the muscle it is considered fibrosis, which is characterized by a transition from collagen III, a plastic collagen that is often involved in remodeling, to collagen I. To determine if this switch is occurring, we stained for collagen III and collagen I. We found that there was some degree of conversion from collagen III to collagen I in all groups except the 0 day and 10 day reinjury. This is understandable because the 0 day injury group regenerates its muscle in the stage-specific manner that produces successful regeneration. There is a potential explanation for the lack of collagen I in the 10 day reinjury group: fresh rounds of the regeneration-degeneration cycle are ongoing – resulting in continued remodeling inhibiting conversion of collagen III to collagen I.

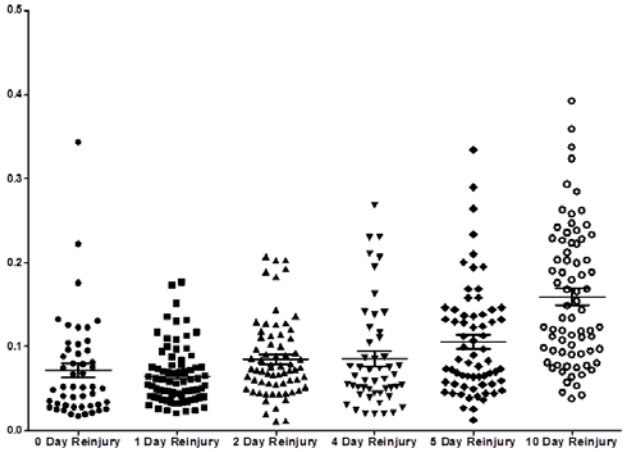

Figure 8. There is an increase in interstitial connective tissue in 10 day reinjury group. y-axis is ratio of fibrosis to total tissue area per field.

6. We have also noticed that two of the samples from the 10 day reinjury group have calcified fibers (Figure 9). We are planning to look further into what their presence means. The calcified fibers are also seen in human DMD muscles.

<u>Further analyses of muscle regions with different regeneration stages induced by repeated injury and the regions in between.</u>

We extensively analyzed the muscle tissues obtained from the regions with the repeated injury by a variety of histological, immunolocalization studies, laser capture microscopy (LCM), microarrays, and enzymatic studies to define the response of neighboring asynchronously remodeling areas, as well as the areas of myofibers in between the two regenerating regions.

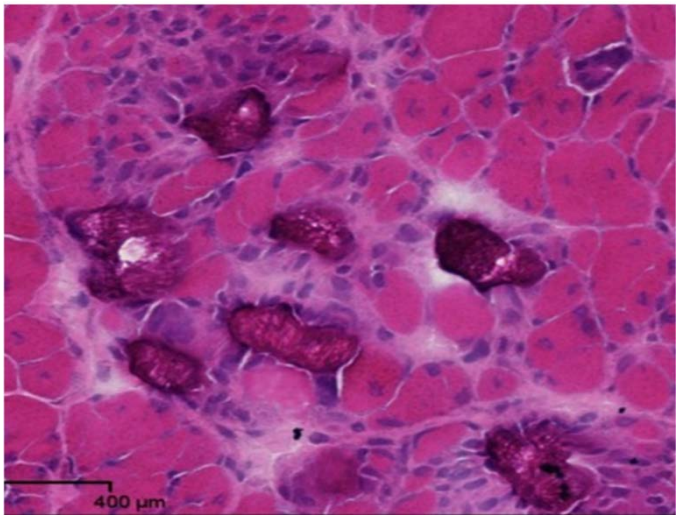

Figure 9. Calcified fibers were seen in 10 day reinjury muscle samples.

Our hypothesis of inappropriate crosstalk predicts that local regions of the muscle tissue may react differently to asynchronous remodeling. We used LCM to dissect the muscles with different regenerating stages. Muscles were dissected from the areas where the red and blue tattoo dyes were in close proximity to each other (e.g. neighboring sites of injections 1 and 2). We focused on the mouse groups of 0 day, 4 days and 10 days between injections. In this experiment, we sacrificed the mice 13 days after the 2nd injection. The 0 day group was used as a control group. The 2nd injection times of the 4 and 10 days series were matched to the distinct phases in normal synchronous regeneration: 4 day time point to myotube formation, and 10 day time point to connective tissue remodeling.

<u>Five regions were excised using LCM from each muscle:</u>

1. Blue dye area (injection 1; 17 days post-injection for the 4 day series; 23 days post-injection for the 10 day series);
2. Red dye area (injection 2; 13 days post-injection for both series);
3. Muscle fibers in between the two injections sites (namely <u>'in between' -- area with potential crosstalk between the two neighboring areas with staged injections</u>);
4. Normal non-regenerating (uninjured) myofibers (identified by peripheral nuclei);
5. Single injection site (single dye area with no evidence of the second dye). These areas were identified by centralized nuclei myofibers located in external area of one injury site (either blue or red).

We isolated RNAs from the LCM excised muscle regions, and profiled mRNAs using Illumina BeadArray chips. We first compared regions 4 (uninjured) vs. region 5 (single regeneration). There were very few differentially

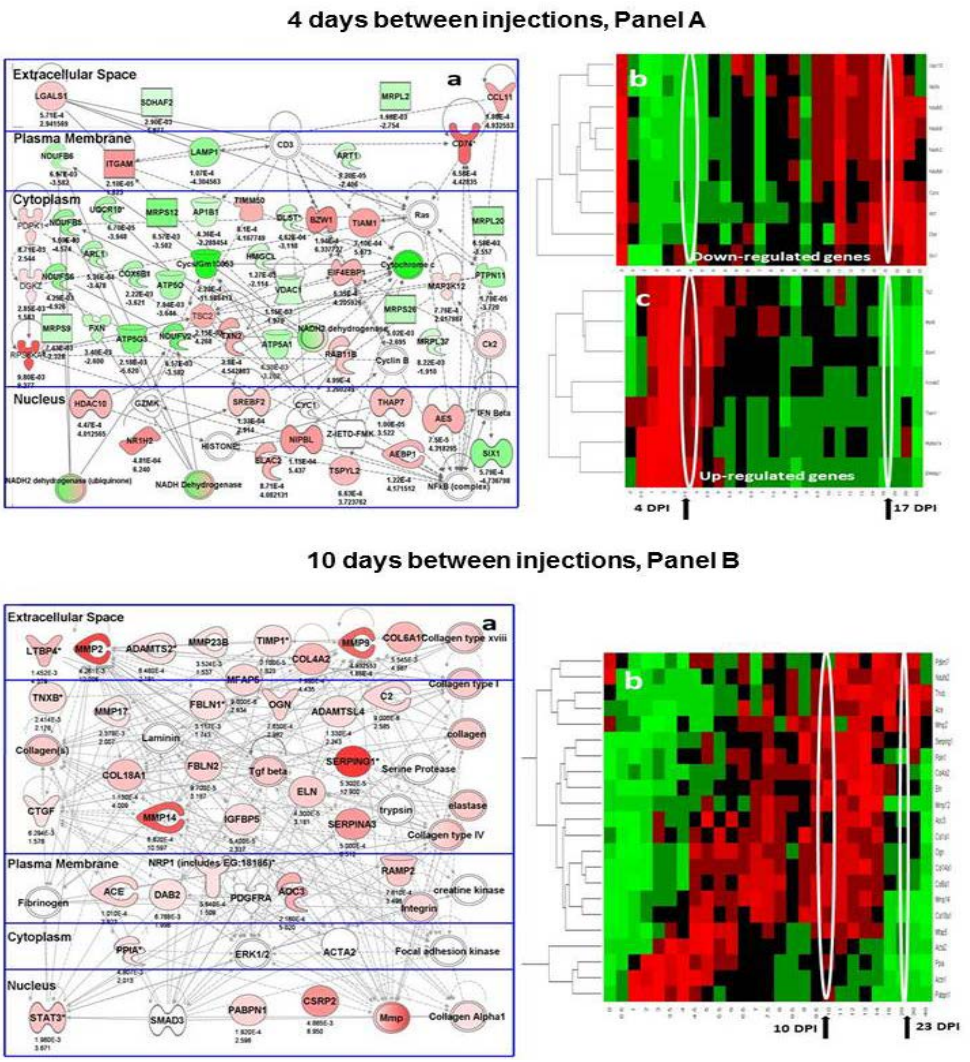

Figure 10. Muscle tissue areas located between the two staged injection sites show evidence of inability to progress appropriately through muscle regeneration. DPI stands for Day Post Injection. LCM was used to isolate regions of myofibers in between injection sites and the two injection sites. Gene expression profiles were generated for these regions, as well as other control regions of the same muscle (non-regenerated wild-type; single site regeneration). Significant expression changes in the intervening regions (in between injection sites) relative to single injection sites were then analyzed. Ingenuity Pathway Analysis was then used to find the significant interaction networks (left panels) affected by the expression changes.

Panel A: The tissue in between the two injection sites of 4 days apart showed down-regulation of mitochondrial function (intracellular) transcripts, and upregulation of extracellular inflammatory transcripts. These transcripts were then mapped against normal synchronous muscle regeneration (Panels b& c), with separate heat maps shown for downregulated transcripts (b) and up-regulated transcripts (c). The white ovals and black arrow points to the time point after the 1st injection that the mice were studied. This showed that the mitochondrial-associated transcripts were expected to have largely recovered to wild-type uninjured control levels by the 27 day time point, but instead were strongly downregulated in the myofibers in between the two injection sites. This pattern was more consistent with the 4 day time point during staged regeneration (white oval and arrow; panel b), suggesting that the intervening region was arrested at the time points between the two injections, and unable to progress appropriately through remodeling. Likewise, the upregulated inflammatory transcripts (extracellular and nuclear red symbols in left panel) were expected to show low levels at the 27 day time point (right white oval, panel c), but instead showed strong upregulation more consistent with the 4 day time point (left white oval).

Panel B: The data for the LCM region of muscle between the injection sites spaced 10 days apart. The organization of Panel B parallels that of Panel A. In the area of muscle in between the two injection sites, there is strong upregulation of fibrosis networks (red symbols) with most appearing in the extracellular space. This was similar to the fibrosis network identified in DMD patient muscle. Mapping of these transcripts against normal staged muscle regeneration showed lack of resolution of these transcripts expected at the later time point at which the mice were sacrificed (white ovals). CD11b (integrin alpha M; ITGM) (panel A) and MMP9 (panel B) were only shown to be differentially expressed under $p < 0.05$ without multiple testing, and FC≤ 1.5 and FC≥ 1.5 statistical analysis criteria. Since these molecules were central to the networks shown, and since mRNA profiling of LCM areas is not expected to be extremely sensitive, we tested for protein expression of these two network members.

expressed genes, suggesting that the muscle in region 5 had indeed successfully regenerated. Likewise, we observed few differentially expressed genes between regions 1 (1st injection) vs. regions 5 (single injection site), and region 2 (2nd injection) vs. region 5, indicating that the regenerations in region 1 and 2 are as successful as region 5. In contrast, the comparison of the in between areas (with potential crosstalk; region 3) in both the 4 day series (Figure 10, Panel A) and the 10 day series (Figure 10, Panel B) showed remarkable mRNA expression profiles. Specifically, the 4 day in between crosstalk area showed a relative loss of mitochondrial-related transcripts and an increase in inflammatory transcripts (Figure 10, Panel A). The 10 day in between crosstalk area showed increase of extracellular matrix components (Figure 10, Panel B). Statistical comparison of fold-changes and p values between the 4 day and 10 day multiple injection sites showed highly significant differences, with the mitochondrial activity alterations specific to the 4 day time series, and the extracellular matrix transcripts specific to the 10 day time series.

We had previously noted that connective tissue transcripts indicative of fibrosis and extracellular matrix remodeling were typically seen in normal muscle regeneration in the myotube maturation stage. As the 10 day staged injection time points were within this window of normal remodeling, we then overlaid the gene networks in Figure 10; Panel B, over normal staged muscle regeneration time series (Figure 10, Panel B-b). For the 4 day injection time points, the downregulated and upregulated transcripts in the in between area were overlaid separately (Figure 10, Panel A-b, A-c). This showed that the downregulated mitochondrial transcripts (Figure 10, Panel A-b) were highly expressed in uninjured and fully regenerated muscle, but were strongly downregulated both in the 4 day in-between area as well as the 4 day time point during normal staged regeneration. This result indicated that the in between area was having arrested regeneration of the 4 day time point. Similarly, the upregulated inflammatory transcripts in the in between area separated by 4 days were highly expressed at the 4 day time point of normal staged regeneration, but not at the later fully regenerated time point (Figure 10, Panel A-c). Thus, both the downregulated mitochondrial transcripts, and the upregulated inflammatory transcripts in the in between area appeared arrested at the time point between the asynchronous injection times.

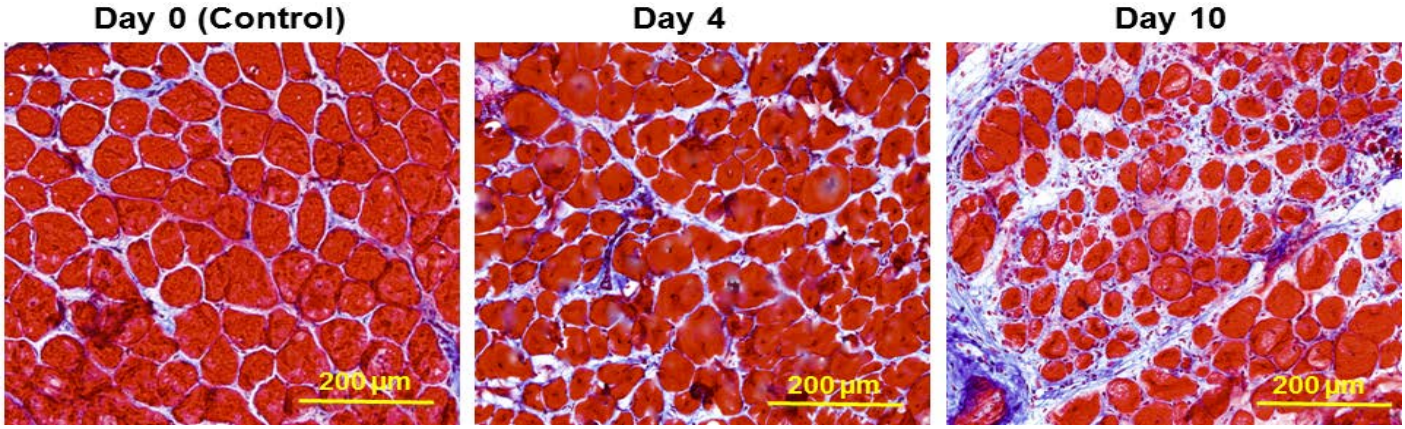

Figure 11. Histologic analysis of connective tissue proliferation (fibrosis). Masson's modified trichrome staining of cryosections in the area of muscle between injection sites staged 0 days (Panel A), 4 days (Panel B), and 10 days (Panel C) apart. Endomysial fibrosis is most evident in the area between injections space 10 days apart (Panel C), consistent with the LCM expression profiling data (Figure 10, Panel B).

The 10 day staged injection series also showed that the in between region has similar phenomenon of arrested development due to neighboring asynchronous regenerations. Connective tissue remodeling transcripts were highly upregulated in the in between area, and this pattern was consistent with the 10 day time point in normal regeneration (Figure 10, Panel B-b). Statistical analysis showed that this pattern was largely specific to the 10 day staged remodeling, and not seen in the 4 day staged remodeling. The microarray data suggested that the 10 day asynchronous remodeling area showed inappropriate persistent expression of connective tissue remodeling transcripts, and this would be consistent with localized tissue fibrosis seen in dystrophic muscles. Histological visualization of the area between the two injection sites showed dramatic fibrotic replacement of muscle in the 10 day series, that was not seen with the 0 day and 4 day series (Figure 11).

Show that daily glucocorticoids result in more successful regeneration in both normal asynchronous regeneration and mdx mice.

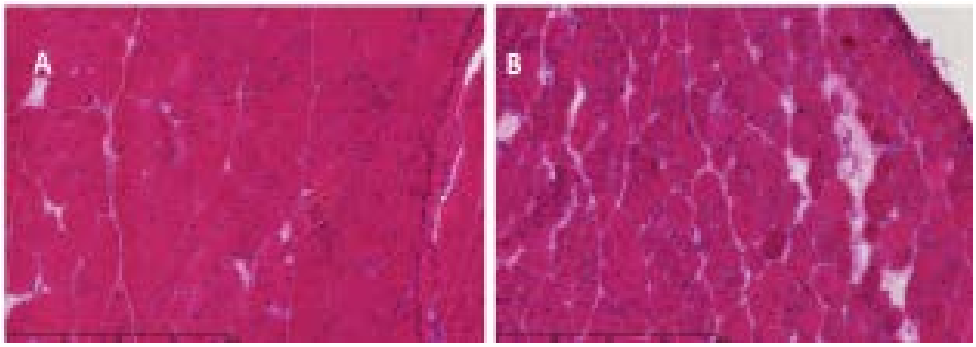

Figure 12. Effect of timing of administering glucocorticoids. The muscles of mice treated at the endogenous circadian nadir (A) results in significantly larger fibers and less inflammation and fibrosis compared to treated at the endogenous circadian peak (B).

We have conducted a study to determine the effects of time of glucocorticoid administration with respect to the animals' endogenous circadian rhythm (we used the light and dark cycle of the animal facility as our benchmark). Animals were treated with prednisone orally at lights ON (circadian nadir) or lights OFF (circadian peak) for five weeks. While we did not see a significant difference in our functional assays, we found histologically that administering glucocorticoids at the animals' endogenous circadian nadir, rather than its endogenous peak, resulted in a significant increase in fiber size and a significant decrease in inflammation and fibrosis (Figure 12). This result has been included in one of our recent publications.[14]

We hypothesized that glucocorticoid drugs may suppress inappropriate crosstalk in the regions between asynchronously remodeling areas of muscle, particularly those associated with the pro-inflammatory 4 day asynchronous crosstalk regions. To test this, we carried out the same asynchronous remodeling experiment using the 4 day time between 1st and 2nd injections, and similarly sacrificing mice 13 days after the 2nd injection, and we used daily administration of Prednisolone (5 mg/kg/day oral) during recovery. Immunostaining of CD11b, CD163 and CD74 (Figure 13) showed the expected expression in the 4 day injection sites. Daily administration of Prednisolone markedly reduced the immunopositivity for these antigens (Figure 14). Control group (without Prednisolone treatments) with induced 1st and 2nd injections at the same time, did not show deferential expression of these genes/proteins that indicate successful regeneration remodeling.

Key Research Accomplishments

1. We have successfully developed and tested the computational genetic network reconstruction algorithms proposed in Aim 1. Using simulation data, we showed that the methods are very effective in reducing noise and estimating regulatory strength and relationship among genes.
2. We have re-profiled rat time series rat acute transcriptional time series of bolus administration of glucocorticoids using Illumina gene expression BeadChip that measures four times of genes relative to the old Affymetrix chip used to generate the existing time series.
3. By integrating our pre-existing multiple muscle transcriptional profiling data sets of human DMD, mouse mdx, and dog GRMD, we have identified a series of commonly shared canonical pathways related to DMD pathogenesis at different age/disease stages across human, mouse and dog. All these pathways (Table 1) are sporadically or not affected at the presymptomatic stage in human, mouse and dog, but they are much more broadly affected at the postsymptomatic stage.
4. We have established staged injection models for inducing asynchronous regeneration in normal mouse muscle. Using LCM and gene expression microarray profiling, we extensively analyzed muscle tissues dissected from the injection sites and in between regions in the 4 day and 10 day injection series. The results showed that inappropriate crosstalk in the muscles from in between areas due to the asynchronous regenerations in both injection series. The phenomena are in part consistent with the pathological phenotypes in Duchenne dystrophic muscles.

5. We showed that daily administration of prednisolone markedly reduced the immunopositivity for antigens CD11b, CD163 and CD74 in the muscles from the in between areas of the 4 day injection series. This suggests that glucocorticoid drugs may suppress inappropriate crosstalk in the muscle regions between asynchronously regeneration areas.
6. We have tested and compared the effect of timing of glucocorticoids administration with respect to the animal's endogenous circadian rhythm. Our results showed significant histological difference in terms of success of muscle recovery from repeated injuries in comparing muscles treated with prednisone orally at lights ON (circadian nadir) or lights OFF (circadian peak) for five weeks. This result implies the connection of the action of glucocorticoid drug and the circadian rhythm.

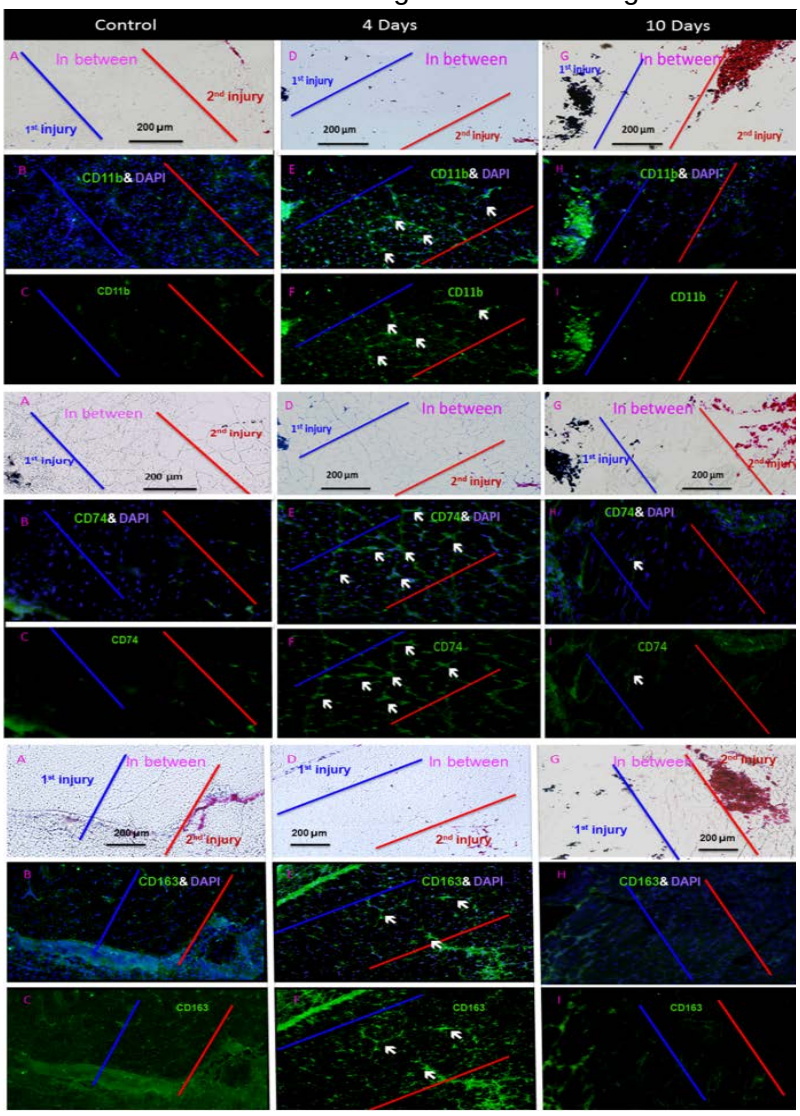

Figure 13. Immunostaining of inflammatory proteins CD11b, CD74 and CD163 showed expression specific to in between areas of muscle between injections spaced 4 days apart.
Panel A: Shown is immunofluorescence of CD11b (Integrin alpha M [ITGAM]). The upper panels show phase microscopy visualization of injection (injury) sites. CD11b is seen highly expressed in the area of muscle in between the injection sites spaced 4 days apart, but not 0 days or 10 days apart. These results are consistent with the LCM expression profiles shown in Figure 10, Panel A.
Panel B: Shown is immunofluorescence of CD74 (HLA class II histocompatibility antigen gamma chain). The upper panels show phase microscopy visualizing the two injection sites labeled with tattoo dyes. CD74 shows high level expression in the area between the injection sites (1st injury, 2nd injury) when injections were spaced 4 days apart, but not in injections space 0 days or noticeably in 10 days apart. These data confirms the LCM expression profiles in Figure 10, Panel A.
Panel C: Shown is immunofluorescence of CD163, cell surface markers of monocytes and macrophages class II (M2c). The upper panel shows phase microscopy visualizing of the repeated injuries and in-between area. Similar to the expression of CD74 and CD11b, CD163 is observed to be highly expressed in the in between area of the 4 days apart model, but not those of 0 days or 10 days apart models.

Reportable Outcomes

1. Evolved from this award, an MDA grant has been awarded, it is a comprehensive project with emphasis on biological validation: Mechanism of steroid action in DMD, grant # 15914, 1/1/2010 – 12/31/2012. The goal is to understand the effects of glucocorticoids on muscle and enable the development of better targeted and more effective therapies for Duchenne muscular dystrophy dynamically. This MDA grant proposal is led by Dr. Eric Hoffman, and it supported a doctoral student's dissertation project.
2. The PI, Dr. Zuyi Wang, was awarded a grant in June 2011 by PPMD (Parent Project Muscular Dystrophy), a private foundation dedicating to DMD research. The purpose of the grant is to prioritize

FDA-approved drugs for human and animal testing for DMD. The work in this grant has strong connections with the newly awarded PPMD grant in many aspects.

3. The PI, Dr. Zuyi Wang, was awarded a pilot grant in February 2011 by Clinical and Translational Science Institute at Children's National (CTSI-CN) funded by NIH CTSA program. This pilot grant focuses on studying glucocorticoids action in treating asthma. Chronic inflammation is a shared feature in many disorders of various tissues (including muscle and lung) for which glucocorticoids provide the standard of care. The PI's research on glucocorticoid action in muscle has provided valuable resources of experiences and methods to the proposed study on asthma.
4. The PI, Dr. Zuyi Wang, received two grants from the Junior Faculty Fund program of Center for Genetic Medicine/Department of Integrative Systems Biology in 2011 and 2012 respectively. The two grants are designed to establish in vitro model for studying the effects of glucocorticoid drugs in human asthmatic airway epithelial cells. This is a systems biology study of molecular effects on glucocorticoid drug action in asthma.

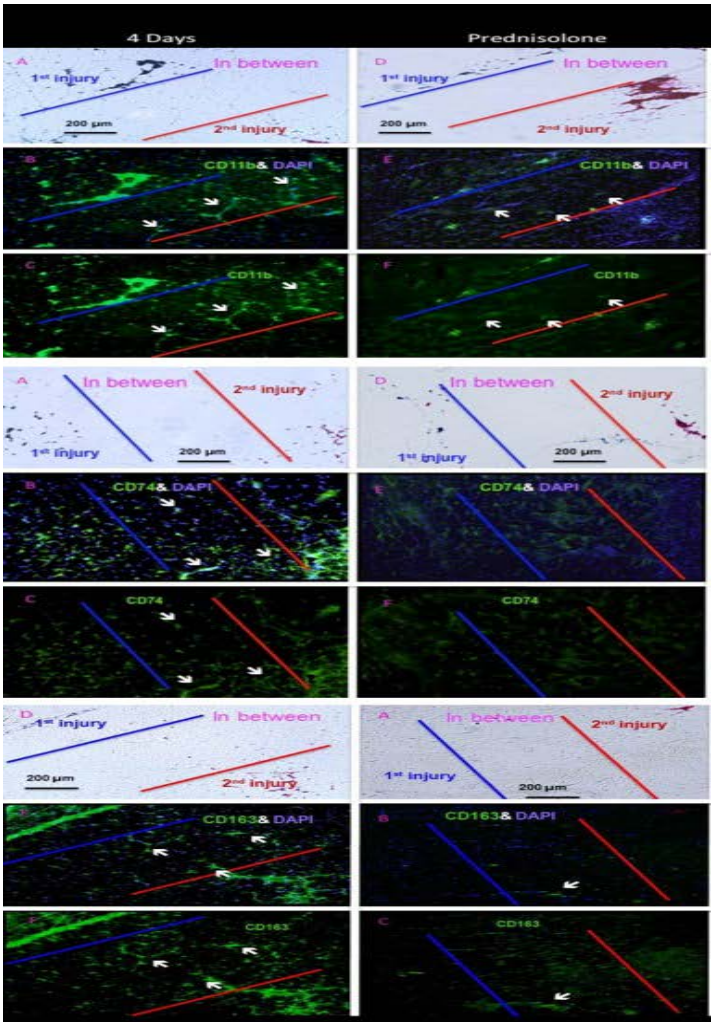

Figure 14. Immunostaining show reduced/ suppressed expression of inflammatory proteins CD11b, CD74 and CD163 in 4 days apart in between area after treatment with prednisolone.

5. L. Fu, R. Freichtat, S. Teach, R. Lorenzo, E. Hoffman, Z. Wang. "Bayesian network analysis suggests ranking of major clinical, behavioral and environmental variables influencing asthma outcomes." American Thoracic Society; 2012; San Francisco, *Am J Respir Crit Care Med*; 2012.
6. A. Baudy, E. Reeves, J. Damsker, C. Heier, L. Garvin, J. McCall, S. Rayavarapu, Z. Wang, J. VanderMeulen, A. Sali, V. Jahnke, S. Dugue, D. DuBois, M. Rose, K. Nagaraju, and E. P. Hoffman. "Δ-9,11 steroidal compounds dissociate NF-κB transrepression from GRE-mediated transactivation." *J Pharmacol Exp Ther.* 2012 Oct; 343(1): 225-32.
7. L. Fu, R. Freichtat, S. Teach, R. Lorenzo, E. Hoffman, Z. Wang. "Identifying Risk Factors and Their Interactions For Reduced Lung Function In Pediatric Asthma, A Bayesian Network Analysis." American Thoracic Society; 2013; Philadelphia, Am J Respir Crit Care Med; May 2013.
8. Dr. Sherry Dadgar, who was partially supported by this grant, has recently defended her doctoral dissertation in June 2013 and obtained her PhD degree in Biology from George Washington University. Her advisor is Dr. Eric Hoffman.
9. Ms. Helen Carey-Johnston, who was partially supported by this grant, is completing her doctoral dissertation, and she expects her PhD degree in Biology from George Washington University in a few months. Her advisor is Dr. Eric Hoffman.

Conclusion

We developed the two proposed computational network reconstruction methods, linear state space model and DBN, to infer transcriptional networks using the rat acute transcriptional time series of bolus administration of glucocorticoids. We have re-profiled the samples of the rat acute transcriptional time series of bolus administration of glucocorticoids using Illumina gene expression BeadChip to obtain a much larger number of measured genes. It is well recognized that reconstructing large scale genetic network is a very complex task. One major obstacle is that the transcriptional microarray data often contain considerable noise that may lead to false estimation of regulatory relationships among genes. We have been testing and comparing the two developed methods on the transcriptional time series data sets about the performance in reliably and correctly reconstructing the regulatory networks. This work is ongoing.

Through integrating multiple muscle data sets of human DMD, mdx and GRMD, we have identified a series of commonly shared canonical pathways related to DMD pathogenesis at different age/disease stages across human DMD, mouse and dog models of DMD. These canonical pathways are very differentially affected at the presymptomatic and postsymptomatic stages, we are studying these pathways and relevant genes to gain in depth understanding of disease progression.

We developed an asynchronous regeneration model for inducing fibrosis and failed regeneration. This model predicted that the normal 2 week regeneration cycle of muscle is disrupted through inappropriate crosstalk between neighboring cells regenerating at different time points of the 2 weak-cycle. To test this hypothesis, we developed an experimental model of focal asynchronous bouts of muscle regeneration, with LCM of marked tissue regions (first bout, second bout, and in between crosstalk areas). Gene expression microarray profiling and immunohistochemical validations showed that the crosstalk areas in between staged bouts of regeneration became inappropriately fixed in the developmental time point by which the initial bouts were separated. This led to a chronic inflammatory state and mitochondrial insufficiency in bouts separated by 4 days, and a chronic pro-fibrotic state in bouts separated by 10 days. Molecular networks associated with these localized areas of pro-inflammatory states were suppressed by treatment with glucocorticoids.

Finally, based on the work accomplished in this grant, we have been awarded several new grants focusing on studying glucocorticoid mechanism in treating DMD and asthma, and published journal articles and conference abstracts. The grant also partially supported two doctoral students' stipend and experiments; one of them graduated in June 2013, and the other one will graduate in a few months.

References

1. Daubechies I. Ten lectures on wavelets. Philadelphia: Society for Industrial and Applied Mathematics; 1992.
2. Mallat S. A Wavelet Tour of Signal Processing. 2nd ed: Academic Press; 1999.
3. Percival DB. Wavelet methods for time series analysis. New York: Cambridge University Press; 2000.
4. Perrin B-E, Ralaivola L, Mazurie A, Bottani S, Mallet J, d'Alche-Buc F. Gene networks inference using dynamic Bayesian networks. Bioinformatics 2003;19:ii138-48.
5. Beal MJ, Falciani F, Ghahramani Z, Rangel C, Wild DL. A Bayesian approach to reconstructing genetic regulatory networks with hidden factors. Bioinformatics 2005;21:349-56.
6. Fujita A, Sato JR, Garay-Malpartida HM, Morettin PA, Sogayar MC, Ferreira CE. Time-varying modeling of gene expression regulatory networks using the wavelet dynamic vector autoregressive method. Bioinformatics 2007;23:1623-30.
7. Heron EA, Finkenstadt B, Rand DA. Bayesian inference for dynamic transcriptional regulation; the Hes1 system as a case study. Bioinformatics 2007;23:2596-603.
8. Kim SY, Imoto S, Miyano S. Inferring gene networks from time series microarray data using dynamic Bayesian networks. Brief Bioinform 2003;4:228-35.
9. Zou M, Conzen SD. A new dynamic Bayesian network (DBN) approach for identifying gene regulatory networks from time course microarray data. Bioinformatics 2005;21:71-9.
10. Neapolitan R. Learning Bayesian Network: Pearson Prentice Hall; 2004.
11. Cooper G. The computational complexity probabilistic inference using belief network. Artificial Intelligence 1990;42:393-405.
12. Holms D. Innovations in Bayesian Networks: Theory and Applications (Studies in Computational Intelligence): Springer; 2010.

13. Fu L, Freishtat RJ, Teach SJ, Resca L, Hoffman EP, Wang Z. Bayesian network analysis suggests ranking of major clinical, behavioral and environmental variables influencing asthma outcomes. In: American Thoracic Society. San Francisco, CA: Am. J. Respir. Crit. Care Med.; 2012.
14. Baudy A, Sali A, Jordan S, et al. Non-invasive optical imaging of muscle pathology in mdx mice using cathepsin caged near-infrared imaging. Mol Imaging Biol 2011;13:462-70.